Available online at www.sciencedirect.com
SCIENCE DIRECT®
Journal of Nuclear Materials 346 (2005) 253–265
journal of nuclear materials
www.elsevier.com/locate/jnucmat

Evolution of the local environment of cerium and neodymium during simplified SON68 glass alteration

Patrick Jollivet [a,*], Christophe Lopez [a], Christophe Den Auwer [a], Eric Simoni [b]

[a] Commissariat à l'Énergie Atomique (CEA), Rhône Valley Research Center, BP 17171, 30207 Bagnols-sur-Cèze, France
[b] Institut de Physique Nucléaire, Bâtiment 100, 91406 Orsay cedex, France

Received 27 April 2004; accepted 27 June 2005

Abstract

The evolution of the sites occupied by cerium and neodymium (coordination numbers and Ce, Nd–O distances) during alteration of simplified SON68 glass specimens was determined by L_{III}-edge XAS. Cerium and neodymium are situated in a silicate environment in the glass, surrounded by eight oxygen atoms at an average distance of 2.44 and 2.48 Å, respectively. These two rare earth elements exhibit different leaching behavior, however. The main environment of cerium becomes a silicate ($d_{Ce–O} = 2.19$ Å) with a second oxide or more probably oxyhydroxide site ($d_{Ce–O} = 2.32$ Å). The cerium coordination number increases by 1 to 3 compared with the glass, depending on the leaching conditions. Neodymium is found mainly in a hydroxycarbonate environment ($d_{Nd–O} = 2.46$ Å); the second site is a silicate ($d_{Nd–O} = 2.54$ Å). The neodymium coordination number increases by 1 compared with the glass. When glass containing neodymium is doped with phosphorus, Nd is situated in a phosphate environment; this change is also reflected in the coordination number and Nd–O distance (seven oxygen atoms at 2.42 Å). During glass leaching, neodymium is present at two different sites, phosphate ($d_{Nd–O} = 2.52$ Å) and hydroxycarbonate ($d_{Nd–O} = 2.40$ Å).

1. Introduction

During leaching of high-level waste containment glass, a surface layer called 'gel' is formed, incorporating a large number of radionuclides – notably the transition metals, the rare earth elements and the actinides. Assuming geological disposal of the glass, radionuclide retention significantly diminishes the activity released from the glass package. In order to take the retention factors into account in safety calculations, its persistence must be demonstrated. This can be achieved by studying the evolution of the local environment of the elements during the glass–gel transformation to determine whether they are incorporated into the silicate network forming the gels. This type of study can yield information concerning the mechanisms of radionuclide incorporation in the gels, as already reported for zirconium [1] iron [1,2], europium [3] and uranium [4,5].

In this paper, we investigate the behavior of the rare earth elements during leaching of simplified SON68-type glass samples with only 9 or 10 constituent elements (SON68 is a non-radioactive glass made of about thirty elements that has the same composition than the R7T7 glass). We selected cerium and neodymium, as these elements are used as surrogates for plutonium and

* Corresponding author. Tel.: +33 4 6679 6373; fax: +33 4 6679 6620.
E-mail address: patrick.jollivet@cea.fr (P. Jollivet).

0022-3115/$ - see front matter © 2005 Elsevier B.V. All rights reserved.
doi:10.1016/j.jnucmat.2005.06.017

americium, because of their oxidation states, ionic radii and electronic structures [6]. The rare earth retention factors in the gels depend on the glass alteration conditions and thus on the nature of the resulting gels. One of the most important parameters of glass alteration in a geological repository is the leaching solution renewal rate. Glass samples were altered with three leachate renewal rates to determine the influence of this parameter on the local environment of cerium and neodymium. More, the influence of the presence of phosphorus in glass on the Nd local environment was also studied because of the high affinity of phosphorus for the rare earth elements. Because of the basically amorphous nature of the gels, the local environment was studied by X-ray absorption spectroscopy (XANES and EXAFS) at the L_{III} absorption edge of cerium and neodymium.

2. Experimental

2.1. Glass compositions

The test specimens were SON68-type glass compositions simplified to only 9 or 10 elements. Three samples doped with 2 wt% or 8 wt% Ce_2O_3 were fabricated in a zirconia crucible at 1100 °C or 1400 °C in a muffle furnace (their compositions correspond to the composition of starting compounds and are indicated in Table 1). The temperature modifies the Ce(III)/Ce(IV) ratio in the glass (68% Ce(III) at 1200 °C and 88% Ce(III) at 1400 °C). Glass sample Ce1 (2 wt% Ce_2O_3) was fabricated at 1200 °C. Sample Ce2, identical to Ce1, was fabricated at 1400 °C, as was sample Ce3, which was doped with 8 wt% Ce_2O_3. Three neodymium-doped glass samples were also fabricated and their compositions are indicated in Table 2. Glasses Nd1 and Nd2 were doped with 1.9 wt% and 3.7 wt% Nd_2O_3. Glass Nd3 was fabricated with the same composition as Nd2, but with the addition of 1.8 wt% P_2O_5 (2 atoms of phosphorus for 1 neodymium). Glasses Nd1 and Nd2 were fabricated at 1200 °C, and sample Nd3 at 1300 °C, for 3 h in a platinum crucible, then annealed for 1 h at 520 °C in a graphite crucible. Glass sample Nd3 appeared opalescent, but SEM analysis did not reveal any heterogeneities.

2.2. Gel fabrication

The test gels were obtained by complete alteration (in pseudo-dynamic mode at 90 °C) of a glass powder comprising only the grain size fraction smaller than 20 μm. The specific surface area of the glass powder was measured by krypton adsorption using the BET method; the mean value was $0.9\,m^2\,g^{-1}$. The leaching solution was water pure (18 MΩcm) and the leachate renewal rates were 2/day, 2/week and 1/week (indicated by the subscripts a, b and c, respectively, in the gel designations). The alteration conditions for the cerium- and neodymium-doped glass specimens are indicated in Tables 3 and 4. The glass alteration times necessary to obtain gels a, b and c were 1 month, 1 year and 3 years, respectively. The glass alteration rates ranged from 0.1 to 0.002 $g\,m^{-2}\,d^{-1}$ (compared with $0.0003\,g\,m^{-2}\,d^{-1}$, the long-term residual alteration rate of SON68 glass at 90 °C). The molar compositions of the cerium- and neodymium-doped gels (Tables 1 and 2) were calculated from the element concentrations analyzed in the leachates. Unlike the neodymium-doped glass, the cerium-doped glass was highly sensitive to differences in the renewal rate, which resulted in significant variations in the gel chemical composition. In gels Ce1a and Ce3a, the major element was thus not silicon but aluminum. The gels obtained with renewal rates of 2/day were highly depleted in silicon and contained only low-solubility elements (Si, Al, Zn, Zr, Ce). The recovered gels were oven-dried at 90 °C for 1 day to eliminate the free pore water from the gel while conserving the structural water. After drying, the gels were press-compacted with cellulose and fixed with Kapton tape. Two additional samples, Nds

Table 1
Molar composition of cerium-doped glass and gels

Element	Glasses			Gels						
	Ce1	Ce2	Ce3	Ce1a	Ce2a	Ce3a	Ce1b	Ce2b	Ce3b	Ce3c
Si	17.52	18.41	18.27	4.11	14.58	7.50	17.54	15.12	15.12	21.97
Al	1.56	1.56	1.59	14.61	8.64	8.71	5.15	8.60	7.47	4.97
B	10.50	9.66	9.31	0.0	0.0	0.0	0.0	0.0	0.0	0.0
Na	4.46	4.19	3.93	0.0	0.0	0.0	0.0	0.0	0.0	0.0
Ca	1.65	1.71	1.69	0.39	0.0	0.0	5.45	2.80	3.38	3.91
Li	3.26	3.06	2.93	0.0	0.0	0.0	0.0	0.0	0.0	0.0
Zn	0.73	0.76	0.76	15.41	11.24	9.92	7.25	8.78	5.22	2.46
Zr	0.13	0.11	0.10	2.56	1.54	1.25	1.24	1.17	0.69	0.32
Ce	0.22	0.23	0.98	4.74	3.03	12.86	2.16	2.59	6.68	3.18
O	59.97	60.31	60.44	58.18	60.97	59.76	61.21	60.94	61.44	63.19

Table 2
Molar composition of neodymium-doped glass and gels

Element	Glasses			Gels						
	Nd1	Nd2	Nd3	Nd1a	Nd2a	Nd3a	Nd1b	Nd2b	Nd3b	Nd2c
Si	18.55	18.14	17.66	20.79	17.80	15.09	18.30	17.29	19.43	20.68
Al	1.55	1.56	1.57	5.37	6.29	6.15	7.80	8.26	5.36	6.96
B	9.57	9.77	9.78	0.0	0.0	0.0	0.0	0.0	0.0	0.0
Na	4.15	4.22	4.22	3.38	3.73	0.0	0.0	0.0	0.0	0.69
Ca	1.68	1.66	1.66	0.0	0.0	4.97	1.66	2.73	5.34	2.34
Li	3.11	3.17	3.18	0.0	0.0	0.0	0.0	0.0	0.0	0.0
Zn	0.74	0.74	0.74	5.85	6.35	4.78	7.20	6.24	3.08	3.83
Zr	0.10	0.10	0.10	0.97	0.93	0.62	0.92	0.11	0.41	0.52
Nd	0.21	0.42	0.42	1.78	3.87	3.26	2.02	3.64	1.76	2.21
P	0.0	0.0	0.89	0.0	0.0	6.23	0.0	0.0	3.69	0.0
O	60.34	60.22	59.78	61.86	61.03	58.90	62.10	61.73	60.93	62.77

Table 3
Characteristics of cerium-doped gels

Parameter	Ce1a	Ce2a	Ce3a	Ce1b	Ce2b	Ce3b	Ce3c
Glass mass (g)	2.0	2.0	2.0	2.5	2.5	2.5	1.0
Leachate volume (L)	1.0	1.0	1.0	0.5	0.5	0.5	0.06
S/V (cm^{-1})	18	18	18	45	45	45	150
Renewal rate	2/day	2/day	2/day	2/week	2/week	2/week	1/week
Alteration rate ($g m^{-2} d^{-1}$)	0.11	0.14	0.13	0.019	0.014	0.028	0.009
Si retention factor	0.01	0.05	0.03	0.10	0.07	0.12	0.37
Ce retention factor	0.92	0.85	0.96	0.98	0.98	0.98	0.99
$pH^{90°}$ start–end	8.4–7.3	8.2–7.2	8.3–7.3	8.7–7.5	8.6–7.8	8.9–7.5	8.2–7.8
[Si] start–end ($mg L^{-1}$)	18–4	17–6	14–5	67–18	38–17	47–4	84–47
Gel mass (g)	0.13	0.15	0.28	0.44	0.28	0.62	0.44

Table 4
Characteristics of neodymium-doped gels

Parameter	Nd1a	Nd2a	Nd3a	Nd1b	Nd2b	Nd3b	Nd2c
Glass mass (g)	2.0	2.0	2.0	2.5	2.5	2.5	1.0
Leachate volume (L)	1.0	1.0	1.0	0.5	0.5	0.5	0.06
S/V (cm^{-1})	18	18	18	45	45	45	150
Renewal rate	2/day	2/day	2/day	2/week	2/week	2/week	1/week
Alteration rate ($g m^{-2} d^{-1}$)	0.050	0.049	0.11	0.012	0.015	0.052	0.0023
Si retention factor	0.11	0.10	0.10	0.10	0.11	0.26	0.21
Nd retention factor	0.84	0.93	0.90	0.98	0.99	0.98	0.96
$pH^{90°}$ start–end	7.6–7.0	7.5–7.1	8.1–7.7	8.8–8.2	8.9–7.9	8.6–7.6	8.2–7.3
[Si] start–end ($mg L^{-1}$)	11–5	11–3	16–4	34–21	16–16	75–21	58–8
Gel mass (g)	0.17	0.48	0.26	0.42	0.47	0.95	0.18

and Ndsp, were fabricated to check for possible differences between the neodymium sites depending on whether it is incorporated in the silicate network of the gel by glass alteration or simply adsorbed. Nds and Ndsp were obtained from sample compositions Nd1 and Nd2 but without neodymium, altered at 90 °C and with 2 renewals per day. The gels were then contacted with a $Nd_2(SO_4)_3 \cdot 8H_2O$ solution at room temperature, resulting in neodymium adsorption on the gel.

2.3. XAS reference compounds

Four cerium and six neodymium model compounds were selected for this study: (i) $CeO_2 \cdot H_2O$ [7] for cerium at oxidation state IV; (ii) $Ce(NO_3)_3 \cdot 6H_2O$ [8], $Ce_2(CO_3)_3 \cdot H_2O$ [9] and $Ce_2Si_2O_7$ [10] for cerium at oxidation state III. $Ce_2Si_2O_7$ was not available for this study. Therefore, the EXAFS spectrum of $Ce_2Si_2O_7$ (averaged over the two crystallographic sites) was

Table 5
Structural parameters of reference compounds

Compound	REE oxidation state	Oxygen number	REE–O distance (Å)	Space group
$Ce(NO_3)_3\cdot 6H_2O$	III	9	2.59	P-1
$Ce_2(CO_3)_3\cdot xH_2O$	III	10	2.42	P-1
$CeO_2\cdot xH_2O$	IV	8	2.34	Fm3m
$Ce_2Si_2O_7$	III	7.5	2.54	P21/c
Nd_2O_3	III	7	2.47	P-3m1
$Nd(OH)_3\cdot xH_2O$	III	9	2.50	$P6_3/m$
$Nd_2(CO_3)_3\cdot xH_2O$	III	9	2.60	Pmcn
$NdPO_4\cdot xH_2O$	III	8	2.46	$P6_222$
$Nd_2Si_2O_7$	III	6.5	2.46	$P2_12_12_1$
$NdOHCO_3$	III	9	2.60	Pmcn

calculated (with FEFF7 code [11]) from the crystallographic data.

For neodymium, Nd_2O_3 [12], $Nd(OH)_3\cdot H_2O$ [13], $Nd_2(CO_3)_3\cdot H_2O$ [14], $NdPO_4\cdot H_2O$ [15], $Nd_2Si_2O_7$ [10] and $NdOHCO_3$ [16] were selected. The two last compounds were not available for this study. Therefore the EXAFS spectrum of $Nd_2Si_2O_7$ (averaged over the two crystallographic sites) and $NdOHCO_3$ were calculated (with FEFF7 code) from the crystallographic data. The crystallographic data of reference compounds are summarized in Table 5.

2.4. XAS data acquisition

The XANES (for Ce only) and EXAFS spectra were recorded at the LURE synchrotron facility (Orsay, France) on the D44 beam line. The beam line is equipped with a double Si(1 1 1) monochromator and borosilicate mirrors in order to remove higher harmonics. Spectra were acquired at the L_{III}-edge of cerium (5723 eV) and neodymium (6208 eV) at room temperature in transmission mode using three air-filled ionization chambers. The third chamber was used for energy calibration of the monochromator: vanadium foil ($E_{max} = 5484.0$ eV) for cerium-doped samples and manganese foil ($E_{max} = 6556.6$ eV) for neodymium-doped samples. Counts were obtained with current intensities ranging from 0.5 to 0.7 nA.

2.5. XAS data treatment

The EXAFS oscillations were extracted by simulating the atomic absorption with a polynomial function (6th degree) (EXAFS98 code [17]). The Fourier-transforms (FT) of the EXAFS spectra were calculated using a k^3-weighted Kaïser window ($\tau = 2.5$) between 2.0 and 10.0 $Å^{-1}$. The local environment of cerium and neodymium was determined after filtering the signal corresponding either to the first coordination sphere (between about 1.4 and 2.5 Å) or the first two spheres (between about 1.4 and 3.8 Å) (distances uncorrected for phase shift) using the RoundMidnight code [17]. The data were weighted with $1/s(k)^2$ where $s(k)$ is the standard deviation of the $k\cdot\chi(k)$ spectra calculated using the EXAFSTAT code [17]. All the experimental spectra were fitted using a zero value for ΔE_0 and a value of 1 for the inelastic electronic loss factor S_0^2.

When the EXAFS spectra of Ce(IV)-doped compounds are extracted, the contributions of the second, third and fourth atomic shells are superimposed on that of the first coordination sphere. These peaks are the result of intense multi-electron excitations [18] and, for the L_{III}-edge, arise from the double transition of the $2p\rightarrow 5d^2$ and $4d\rightarrow 5d^2$ electrons. The contribution of the other atomic shells must therefore be subtracted [19] to obtain the EXAFS signal due exclusively to the first coordination sphere (oxygen atoms). The contribution due to multi-electron excitations has therefore been subtracted from all EXAFS spectra included in this article. Electronic parameters (phases and amplitudes, electron mean free path) were obtained from FEFF7 calculations based on reference compounds.

3. Local environment of cerium in the glasses and gels

3.1. XANES spectra

The L_{III}-edge XANES spectrum of reference compounds $Ce_2(CO_3)_3$ (Ce(III)) exhibits a single peak at about 5728 eV and CeO_2 (Ce(IV) includes two peaks at 5733 and 5740 eV) are shown in Fig. 1. The spectra for glasses Ce1 and Ce2 are also compared and indicate the simultaneous presence of Ce(III) and Ce(IV) in these compounds, but in different proportions (32% and 12% Ce(IV), respectively, obtained by chemical titration). Conversely, the spectrum of gel Ce1a clearly shows the presence of only Ce(IV). All the spectra of the seven gels are identical, and Ce is only present at oxidation state

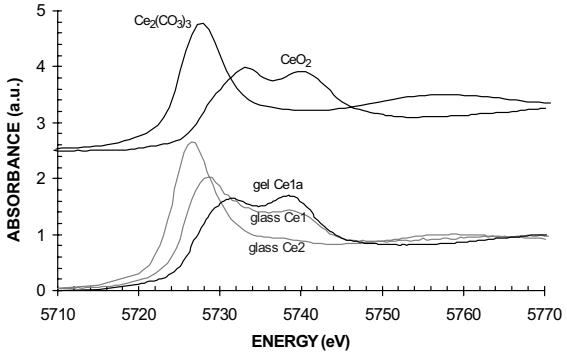

Fig. 1. Cerium L_{III}-edge XANES spectra of glasses Ce1 and Ce2 and gel Ce1a.

IV. This result was expected since the gels were obtained under aerobic conditions and the Eh-pH diagram of cerium [20] indicates that oxidation state IV predominates.

The energy difference between the two white line absorption peaks of Ce(IV) can provide information about the chemical environment of cerium. The energy difference between the two absorption peaks of Ce(IV) is proportional to the Ce–O distance [21]. The difference is 7 eV for all the gels, indicating similar Ce–O distances in all these compounds.

3.2. EXAFS spectra of the glass samples

Comparison of the EXAFS spectra of glass samples Ce1, Ce2 and Ce3 (Fig. 2) reveals no difference up to 10 $Å^{-1}$. The presence of different quantities of Ce(IV) (32% and 12%) in the glass thus does not lead to any visible difference in the spectra. Moreover, none of the glass spectra show any similarity with those of the reference compounds. In Fig. 3, the corresponding radial distribution function (RDF), in the case of Ce3, (distances uncorrected for phase shift) obtained by a Fourier transform of the EXAFS spectra shows a single contribution centered on 1.9 Å due to the first-neighbor oxygen atoms around the cerium atom. There is no signal corresponding to second neighbors in the glass, indicating that the cerium second coordination sphere is made of scattered light atoms (Si, Al, etc.). The EXAFS and RDF spectra of Ce1 and Ce2 are the same than Ce3 one.

A qualitative comparison of the EXAFS spectra of the glasses and reference samples suggests that the cerium environment in the glass is of silicate-type. This means that the cerium first coordination sphere is similar to that in $Ce_2Si_2O_7$. First, the EXAFS spectra of glasses were fitted with the phases and amplitudes from the first

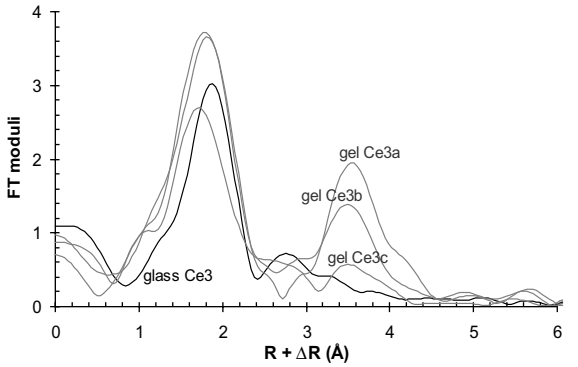

Fig. 3. Radial pseudo-distance distribution in glass Ce3 and gels Ce3a, Ce3b and Ce3c.

coordination sphere of a CeO_2- and $Ce_2(CO_3)_3$-type site, but that led to a bad adjustment, as indicated in Fig. 4. That is why the experimental spectra were fitted on the assumption of a silicate-type site made of a single averaged shell of oxygen atoms. The EXAFS spectrum of the cerium(III) silicate was calculated using the FEFF7 code with cerium atom at the center of two sites. The two simulated spectra were then averaged to extract the phase and amplitude of $Ce_2Si_2O_7$. The adjustments of the glass spectra fitted under these conditions were very satisfactory (Fig. 4) with comparable values for all the glass structural parameters, as indicated in Table 6. The cerium atom in the glass is thus surrounded by 8.2 ± 1.6 oxygen atoms at a mean distance of 2.44 ± 0.02 Å. No bibliographical data are available concerning the local environment of cerium in glass. Only a recent study of natural garnets [22] formed in carbonate rocks showed that cerium incorporated in trace amounts in these

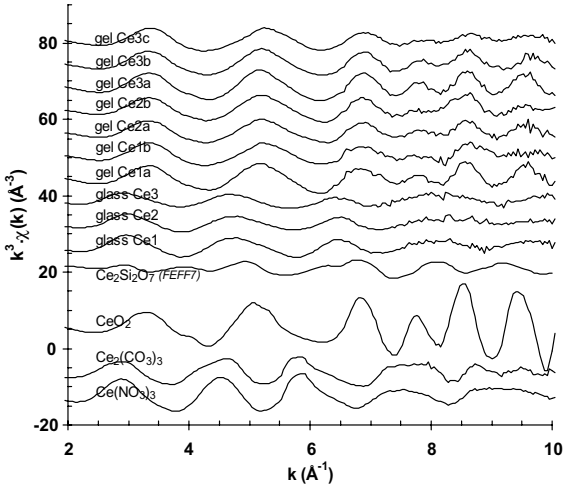

Fig. 2. Cerium L_{III}-edge EXAFS spectra of reference compounds, glasses and gels.

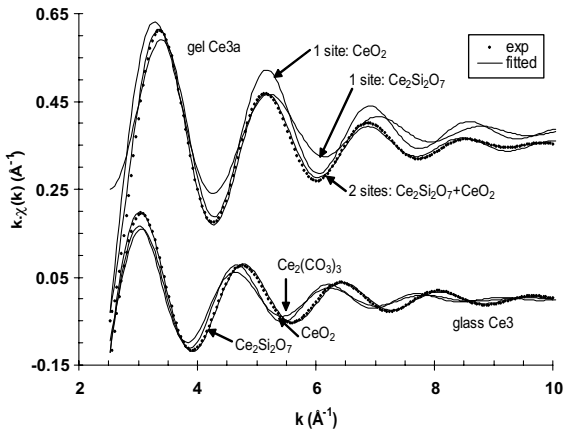

Fig. 4. Comparison between experimental and fitted EXAFS spectra for the first coordination sphere (Ce–O) of glass Ce3 and gel Ce3a.

Table 6
Structural fitting parameters of EXAFS spectra for the first coordination sphere (Ce–O) of cerium-doped materials (F_i and N_i represent the fraction and coordination number of site i; N_T represents the total coordination number)

Material	Site	$N_i \times F_i$	N_T	σ_i (Å)	R_i (Å)	r factor (fit)
Glass Ce1	$Ce_2Si_2O_7$		8.2 ± 1.6	0.048 ± 0.001	2.44 ± 0.02	0.01
Gel Ce1a	$Ce_2Si_2O_7$	6.6 ± 1.3	10.3 ± 2.1	0.061 ± 0.009	2.21 ± 0.02	0.01
	CeO_2	3.7 ± 0.7		0.073 ± 0.008	2.33 ± 0.02	
Gel Ce1b	$Ce_2Si_2O_7$	6.2 ± 1.2	8.3 ± 1.7	0.069 ± 0.002	2.21 ± 0.02	0.01
	CeO_2	2.1 ± 0.4		0.060 ± 0.009	2.31 ± 0.02	
Glass Ce2	$Ce_2Si_2O_7$		8.0 ± 1.6	0.061 ± 0.004	2.44 ± 0.02	0.03
Gel Ce2a	$Ce_2Si_2O_7$	5.9 ± 1.2	9.1 ± 1.8	0.088 ± 0.008	2.19 ± 0.02	0.01
	CeO_2	3.2 ± 0.6		0.077 ± 0.005	2.32 ± 0.02	
Gel Ce2b	$Ce_2Si_2O_7$	6.2 ± 1.2	9.6 ± 1.9	0.084 ± 0.009	2.19 ± 0.02	0.01
	CeO_2	3.4 ± 0.7		0.061 ± 0.013	2.31 ± 0.02	
Glass Ce3	$Ce_2Si_2O_7$		8.3 ± 1.7	0.059 ± 0.002	2.43 ± 0.02	0.02
Gel Ce3a	$Ce_2Si_2O_7$	6.8 ± 1.4	11.1 ± 2.2	0.102 ± 0.008	2.17 ± 0.02	0.01
	CeO_2	4.3 ± 0.9		0.076 ± 0.005	2.32 ± 0.02	
Gel Ce3b	$Ce_2Si_2O_7$	5.7 ± 1.1	9.6 ± 1.9	0.064 ± 0.002	2.19 ± 0.02	0.01
	CeO_2	3.9 ± 0.8		0.071 ± 0.002	2.32 ± 0.02	
Gel Ce3c	$Ce_2Si_2O_7$	5.8 ± 1.2	8.7 ± 1.7	0.055 ± 0.006	2.20 ± 0.02	0.01
	CeO_2	2.9 ± 0.6		0.075 ± 0.006	2.32 ± 0.02	

materials has a coordination number of 8 and a mean Ce–O distance of 2.45 Å. These values are very comparable to those found in our relatively complex glass samples.

3.3. EXAFS spectra of the gel samples

The cerium L_{III}-edge EXAFS spectra of the gels show four significant oscillations at 6.9, 7.8, 8.6 and 9.6 $Å^{-1}$ (Fig. 2). The initial Ce(III)/Ce(IV) ratio in the glass has no effect on the gel spectra. Conversely, the influence of the renewal rate is very clear on gel Ce3. The higher the rate, the more intense the oscillation at 9.6 $Å^{-1}$.

The radial distribution functions (distance uncorrected for phase shift) of the gel (Fig. 3) all show two main peaks due to the first and second neighbors of cerium. The contribution centered on 3.5 Å is observed for all the gels but Ce1b and Ce3c. The higher the leachate renewal rate, the larger the intensity of the second-neighbor contribution. It is thus likely that cerium aggregation occurs during alteration at high flow rates, forming small cerium(IV) oxide or oxyhydroxide entities in the gel silicate network. These particles must be very small (less than 1 μm), however, as they are not observed by SEM. Moreover, X-ray diffraction images show that the gels are mainly amorphous. The patterns of gels Ce3a,b,c (Fig. 5) show two small peaks at 33.9° and 60.3° (2θ) but their intensities are too low to be associated with an accurate compound. The pattern of gel Ce2a includes three low-intensity diffraction lines that may be associated with a mixed cerium and aluminum oxide. The Ce–Ce contribution was observed in gels Ce2b and Ce3b, but not in Ce1b. The presence of Ce(IV) in the glass thus appears to favor the formation of cerium-enriched particles in the gels. The same phenomenon was observed for high cerium concentrations in the glass. This could be attributable to a higher cerium concentration (four times higher in glass Ce3) that would result in earlier cerium saturation of the solution. A larger quantity of cerium would thus have precipitated in gels Ce3a and Ce3b. The lower rate of formation of gel Ce3c could lead to better cerium loading in the silicate network of this gel by diminishing the cerium release from the glass.

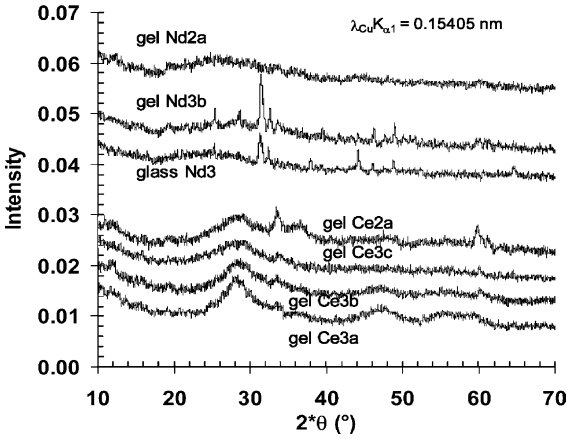

Fig. 5. X-ray diffraction patterns of Nd3 glass and of Ce2a, Ce3a, Ce3b, Ce3c, Nd2a, Nd3b gels.

Although the EXAFS spectra of the gels are qualitatively comparable to the one of CeO_2, cerium probably occupies two types of sites in the gels, as already shown

from lifetimes of europium by a TRLFS (time resolved laser fluorescence spectroscopy) study [3]. Gel spectra fitted with $k \cdot \chi(k)$ filtering for a single type of site resulted in bad amplitudes for CeO_2 and in a phase shift for $Ce_2Si_2O_7$, as indicated by Fig. 4. Conversely, allowing for two types of sites (silicate and oxide) for cerium results in very good agreement between the fitted and experimental spectra (Fig. 4). Similar types of sites (Ce^{3+}, Ce^{4+} and CeO_2) were taken into account to fit the cerium L_{III}-edge XANES spectra [23] for American nuclear waste containment glass. For the silicate site, we used the electronic parameters of $Ce_2Si_2O_7$ since the cerium(IV) silicate structure is not documented in the literature.

Two types of sites are needed to fit the gel spectra. Because the uncertainty relative to the amplitude functions in EXAFS is relatively high, it is difficult to extract absolute value of coordination numbers when two types of sites are needed. However, it is possible to give the evolution of the coordination mode within a series, every thing else being equal. The gel structural parameters for the first coordination sphere (Ce–O bonds) are indicated in Table 6. A variation is observed in the total coordination number of cerium, from 8 ± 1.6 to 11 ± 2.2 (Table 6), depending on the leachate renewal rate and thus on the nature of the gels. However, coordination number determination in EXAFS must be taken with care, especially in the case of a highly disordered system like glasses and gels. The leachate renewal rate had no effect on gels Ce2a and Ce2b, but a major effect in the case of Ce1a and Ce1b. This is probably attributable not to the effect of the Ce(III)/Ce(IV) ratio but to the fact that although gels Ce2a and Ce2b were formed at different flow rates, they had relatively similar chemical compositions and in particular the same silicon concentration. A high leaching solution flow rate thus generally results in strongly hydrated cerium sites (the coordination number increases by about a number of 2 compared with a low flow rate). The cerium concentration in the glass has no influence, as the coordination number is the same in gels Ce2b and Ce3b.

The Ce–O interatomic distances vary little from one gel to another, despite variations in the cerium coordination number. The distances varied between 2.17 and 2.21 Å for the silicate site, versus only 2.31 and 2.33 Å for the oxide site. The Ce–O distances in the gels were much shorter than in the glass, where they were equal to 2.44 Å. The mean distance of the oxide site was 2.32 Å, which is very near the Ce–O distance in CeO_2. This seems to confirm the presence of cerium oxide particles in the gels, although they appear dispersed throughout the gel since no heterogeneities were revealed by electron microscopy. For the silicate sites, the mean distance is 2.19 Å, about 0.25 Å less than in the glass. The difference between the ionic radii of Ce^{3+}(VIII) and Ce^{4+}(VIII) is only 0.17 Å [24]; the difference of 0.25 Å thus cannot be attributed to the presence of Ce^{3+} in the glass and Ce^{4+} in the gels – especially since the difference in the ionic radii ($Ce^{3+} - Ce^{4+}$) diminishes as the Ce^{4+} coordination number increases. Moreover, the difference in the Ce–O bond length in $Ce(H_2O)_n^{3+}$ and $Ce(H_2O)_n^{4+}$ (where $n \sim 9$) is 0.07 Å [25]; this confirms that the variation in the Ce–O bond length between the glass and gels cannot be due exclusively to the change in the cerium oxidation state as a results of glass alteration. There is a large distortion of the first coordination sphere of cerium in the gels compared to the ordered cerium silicate $Ce_2Si_2O_7$ site (difference of 0.35 Å). However, it is not possible to obtain a good fit of the gel spectra using only one type of site ($Ce_2Si_2O_7$ or CeO_2) with two oxygen shells. This difference between the Ce–O distances in the glass and gels thus suggests a major reorganization of the cerium silicate sites during glass alteration.

During leaching, Ce1 glass presents a different behavior from Ce2 and Ce3 glasses one. For Ce1ab gels, the percentage of silicate-type sites increases from 60% to 80% when the renewal rate decreases from 2/day to 2/week. Conversely, this percentage of silicate-type sites is constant at about 60% for Ce2ab and Ce3abc gels, whatever the renewal rate. This could be explained by the fact that the solubility of cerium in solution is quickly reached, even for low flow rates of leaching, because of the larger cerium (III) content in Ce2 and Ce3 glasses.

The Fourier-transforms of the EXAFS spectra (Fig. 3) show that the gels formed at a renewal rate larger or equal to 2/week exhibit a Ce–Ce contribution around 4 Å. The cumulative signal corresponding to the first two coordination spheres around cerium was filtered. The structural parameters obtained for the first coordination sphere were maintained constant; only the second coordination sphere was fitted. To obtain a proper fit of the experimental spectra, as shown in Fig. 6, the second atomic shell – like the first – must be considered as a mixture of silicate ($Ce_2Si_2O_7$) and oxide (CeO_2) sites. An average Ce–Ce distance of about 3.9 Å has been determined (in order to be consistent with the adjustments of the first coordination sphere, this distance corresponds to the average of Ce–Ce contribution in both oxide- and silicate-type of site). This result contrasts with the cerium local structure in the glasses (no visible Ce–Ce contribution) and indicates that upon leaching, major structure rearrangements occur. The error given in Table 7 corresponds to the statistical error associated with the data fitting. Because, these contributions correspond to second sphere neighbors, the effective error on the structural parameters is supposed to be much larger and also very difficult to estimate. The second coordination sphere of Ce1a gel is composed of 2 more times atoms (Table 7) than Ce2ab and Ce3ab ones. The leaching of high cerium content

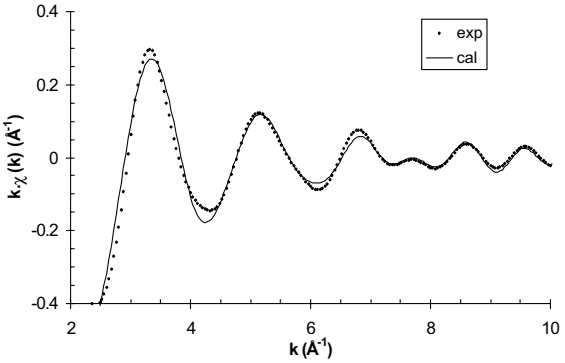

Fig. 6. Comparison between experimental and fitted EXAFS spectrum of gel Ce3a including the first and second coordination spheres (Ce–O + Ce–Ce).

glasses leads to roughly identical second coordination spheres. The environment in the Ce1a gel is close to that of the model compound CeO_2 (12 cerium atoms at 3.83 Å), confirming the presence of small aggregates highly enriched in cerium in the gels.

Cerium is found in a pure silicate environment in the glass, but as silicate and oxide – or more likely oxyhydroxide – sites in the gels. Phases highly enriched in cerium are dispersed throughout the silicate network of the gels. The formation of these phases ceases at low leaching solution flow rates. The presence of CeO_2 sites indicates that cerium is incorporated in the gel silicate network by a dissolution–precipitation mechanism. Moreover, a study of the cerium local environment during Na^+–Ce^{4+} substitution in montmorillonite [26] indicated about eight oxygen atoms at a distance of 2.31 Å, three others at 2.66 Å and about two cerium atoms at 3.78 Å. The 2.31 and 3.78 Å distances correspond to the distances found for the oxide site in our cerium-doped gels. A fraction of the cerium could thus be retained in the gel by ion exchange.

4. Local environment of neodymium in the glasses and gels

4.1. EXAFS spectra of the glass samples

Fig. 7 displays the EXAFS spectra of neodymium reference compounds and glasses. The EXAFS spectra of glass samples Nd1 and Nd2 are identical but the spectrum of glass Nd3 differs from those of Nd1 and Nd2 (without phosphorus), considering the beating modification at 6.7 $Å^{-1}$. Adding phosphorus thus modifies the nature of the sites occupied by neodymium in the glasses. For the glasses without phosphorus, there is no similarity with any of the reference compounds but the EXAFS spectrum of glass Nd3 looks like $NdPO_4$ one, except the beat at 9.0 $Å^{-1}$. Silicon is the main chemical element in the glasses, and it is reasonable to assume a silicate environment for neodymium, at least for the glasses that does not contain phosphorus. Fig. 8 shows the FT of the EXAFS spectra for Nd2 and Nd3. The fact that no signal is observed for the second neighbors (between 3 and 4 Å) indicates that the second neighbors of neodymium are light atoms (Si, P, B and Al). The X-ray diffraction pattern of the glass sample Nd3 (Fig. 5) indicates that this compound is mainly amorphous with a few low-intensity diffraction lines that can be attributed to a mixed calcium and neodymium oxide phosphate. SEM-EDS analysis also showed no variation in the element concentrations in the Nd3 glass sample. The Nd L_{III}-edge EXAFS spectra of $Nd_2Si_2O_7$, $K_3NdSi_2O_7$ and $NaNdSiO_4$ (Fig. 7) were simulated using the FEFF7 code based on their crystallographic coordinates as for the cerium case.

A qualitative comparison of the spectra of Nd1 and Nd2 with $Nd_2Si_2O_7$ one suggests a silicate environment in the glasses without phosphorus. The experimental spectra of the glasses without P were fitted on the assumption of a $Nd_2Si_2O_7$-type site comprising a single averaged shell of oxygen atoms. In this compound, neodymium is present in two crystallographic sites [10]. The

Table 7
Structural fitting parameters of EXAFS spectra for the second coordination sphere (Ce–Ce) of cerium-doped materials (F_i and N_i represent the fraction and coordination number of site i; N_T represents the total coordination number)

Material	Site	$N_i \times F_i$	N_T	σ_i (Å)	R_i (Å)	r factor (fit)
Gel Ce1a	$Ce_2Si_2O_7$	5.8 ± 1.2	9.6 ± 1.9	0.065 ± 0.002	3.97 ± 0.02	0.03
	CeO_2	3.8 ± 0.8		0.072 ± 0.011	3.76 ± 0.02	
Gel Ce2a	$Ce_2Si_2O_7$	1.5 ± 0.3	3 ± 0.6	0.065 ± 0.003	3.93 ± 0.02	0.05
	CeO_2	1.5 ± 0.3		0.056 ± 0.002	3.81 ± 0.02	
Gel Ce2b	$Ce_2Si_2O_7$	2.2 ± 0.4	4.3 ± 0.9	0.063 ± 0.001	3.94 ± 0.02	0.05
	CeO_2	2.1 ± 0.4		0.069 ± 0.006	3.78 ± 0.02	
Gel Ce3a	$Ce_2Si_2O_7$	2.2 ± 0.4	5.9 ± 1.2	0.063 ± 0.006	3.95 ± 0.02	0.02
	CeO_2	3.7 ± 0.7		0.072 ± 0.001	3.79 ± 0.02	
Gel Ce3b	$Ce_2Si_2O_7$	2.5 ± 0.5	5.4 ± 1.1	0.065 ± 0.025	3.93 ± 0.02	0.04
	CeO_2	2.9 ± 0.6		0.082 ± 0.006	3.76 ± 0.02	

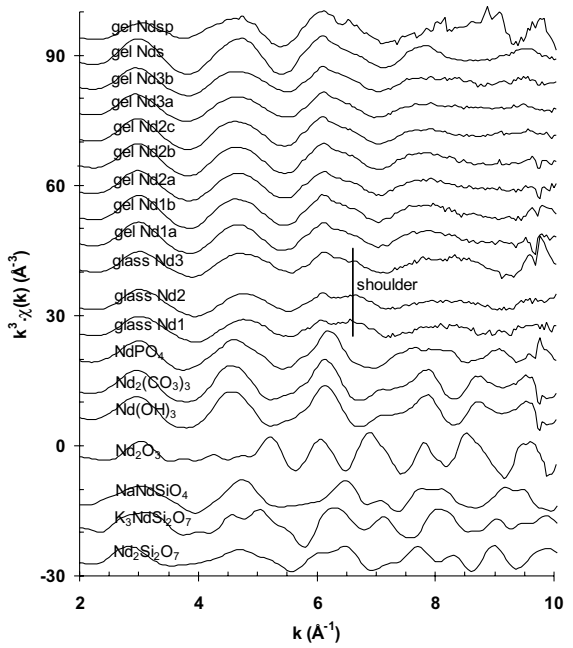

Fig. 7. Neodymium L_{III}-edge EXAFS spectra of model compounds, glasses and gels.

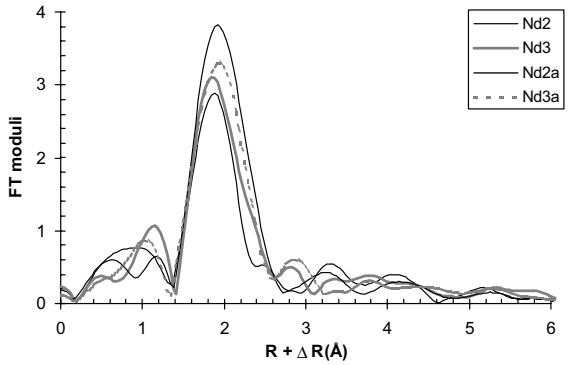

Fig. 8. Radial pseudo-distance distribution in glasses Nd2 and Nd3 and in gels Nd2a and Nd3a.

two simulated (FEFF7) spectra corresponding to each site were then averaged to extract the phase and amplitude of $Nd_2Si_2O_7$. The adjustment of the glass spectra Nd1 and Nd2, fitted with this type of site, are very satisfactory (Fig. 9) with identical values for the Nd1 and Nd2 structural parameters (Table 8). Neodymium in the glass without phosphorus is thus surrounded by 8.2 ± 1.6 oxygen atoms at a mean distance of 2.48 ± 0.02 Å. The scarce published studies of very simplified glasses are relatively contradictory. A study of (SiO_2, B_2O_3, Al_2O_3) glass containing no alkalis [27] showed that Nd is surrounded primarily by borate sites at low neodymium concentrations. Another study of a

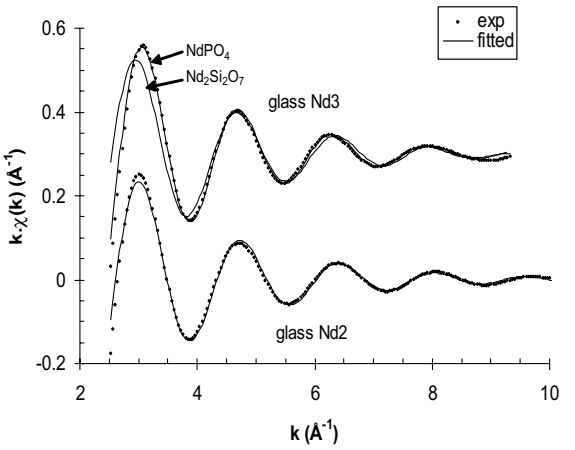

Fig. 9. Comparison between experimental and fitted EXAFS spectra for glasses Nd2 (1 $Nd_2Si_2O_7$ site) and Nd3 (1 $NdPO_4$ or $Nd_2Si_2O_7$ site).

(SiO_2, Al_2O_3) glass [28] showed that Nd could have a charge-compensating role for AlO_4^- entities, and that adding aluminum to the glass significantly increased the Nd–O distance compared with the silicate (2.35 Å). Another study of (Na_2O, SiO_2) glass [29] reported a shorter Nd–O distance when the Nd coordination number increased in glass containing different neodymium concentrations. A study of natural garnets [22] formed in carbonate rocks showed that neodymium incorporated in trace amounts in these materials had a coordination number of 8 and a mean Nd–O distance of 2.43 Å. However, a study of simplified 8-element SRL glasses [30] doped with praseodymium indicated a Pr–O distance of 2.49 Å with about 8 ± 2 oxygen neighbors. These values are identical with our findings for neodymium-doped glass.

The EXAFS spectrum of glass sample Nd3 (that exhibits the characteristic oscillations of neodymium phosphate but the beat at 9.0 $Å^{-1}$) was therefore fitted assuming a $NdPO_4$ site using the phase and amplitude calculated with FEFF7 code from $LaPO_4$ crystallographic data. The resulting fit was very satisfactory (Fig. 9). If a silicate site is considered instead of a phosphate site, it is impossible to obtain a proper fit of the Nd3 glass spectrum. This indicates that phosphate groups form the majority of neodymium first coordination sphere. This is in agreement with the large thermodynamic stability of lanthanide phosphate compounds [31]. In glass sample Nd3, neodymium is surrounded by 6.7 ± 1.3 oxygen atoms at a distance of 2.42 ± 0.02 Å. A study of $(Ln_2O_3)_x(P_2O_5)_{1-x}$ glasses [32] showed that the coordination number of the rare earth elements diminished from 8 to 6 between the ultraphosphates ($x < 0.15$) and metaphosphates ($x \sim 0.25$). Another study of the same type of material [33] also showed that the neodymium coordination number

Table 8
Structural fitting parameters of EXAFS spectra of neodymium-doped materials (F_i and N_i represent the fraction and coordination number of site i; N_T represents the total coordination number)

Material	Site	$N_i \times F_i$	N_T	σ_i (Å)	R_i (Å)	r factor (fit)
Verre Nd1	$Nd_2Si_2O_7$		8.3 ± 1.7	0.054 ± 0.001	2.48 ± 0.02	0.03
Gel Nd1a	$Nd_2Si_2O_7$	3.2 ± 0.7	9.4 ± 1.9	0.085 ± 0.004	2.54 ± 0.02	0.01
	$NdOHCO_3$	6.2 ± 1.3		0.066 ± 0.001	2.45 ± 0.02	
Gel Nd1b	$Nd_2Si_2O_7$	3.6 ± 0.7	9.1 ± 1.8	0.072 ± 0.001	2.53 ± 0.02	0.02
	$NdOHCO_3$	5.5 ± 1.1		0.052 ± 0.002	2.46 ± 0.02	
Verre Nd2	$Nd_2Si_2O_7$		8.0 ± 1.6	0.050 ± 0.006	2.48 ± 0.02	0.05
Gel Nd2a	$Nd_2Si_2O_7$	2.5 ± 0.5	9.0 ± 1.8	0.074 ± 0.007	2.53 ± 0.02	0.01
	$NdOHCO_3$	6.5 ± 1.3		0.073 ± 0.007	2.46 ± 0.02	
Gel Nd2b	$Nd_2Si_2O_7$	3.8 ± 0.8	9.3 ± 1.9	0.061 ± 0.008	2.54 ± 0.02	0.01
	$NdOHCO_3$	5.5 ± 1.1		0.054 ± 0.005	2.45 ± 0.02	
Gel Nd2c	$Nd_2Si_2O_7$	4.7 ± 0.9	9.4 ± 1.9	0.087 ± 0.001	2.53 ± 0.02	0.01
	$NdOHCO_3$	4.7 ± 0.9		0.054 ± 0.001	2.46 ± 0.02	
Verre Nd3	$NdPO_4$		6.7 ± 1.4	0.087 ± 0.003	2.42 ± 0.02	0.01
Gel Nd3a	$NdPO_4$	3.9 ± 0.8	7.9 ± 1.6	0.050 ± 0.001	2.52 ± 0.02	0.01
	$NdOHCO_3$	4.0 ± 0.8		0.049 ± 0.001	2.40 ± 0.02	
Gel Nd3b	$NdPO_4$	3.9 ± 0.8	7.8 ± 1.6	0.063 ± 0.001	2.52 ± 0.02	0.03
	$NdOHCO_3$	3.9 ± 0.8		0.043 ± 0.002	2.40 ± 0.02	
Gel Nds	$NdOHCO_3$		11.0 ± 2.2	0.078 ± 0.001	2.45 ± 0.02	0.01
Gel Ndsp	$NdOHCO_3$		6.7 ± 1.3	0.049 ± 0.002	2.46 ± 0.02	0.01

dropped from 9 to 6.4 when the glass composition varied from ultraphosphate to metaphosphate. The rare earth coordination number is 9 in monazite [34], while the Nd–O bond length diminishes from 2.40 to 2.37 Å. Given the Nd3 glass composition, neodymium must thus be in a metaphosphate environment, and this is indeed the case since the Nd coordination number is 6.7 in Nd3 glass. The fact that the Nd–O bond length in Nd3 glass is 0.05 Å longer than in a neodymium metaphosphate is attributable to the complexity of the glass and to an x value of about 0.5 – considerably higher than for the metaphosphates studied.

4.2. EXAFS spectra of the gel samples

The EXAFS spectra of the gels (Fig. 7) show no differences among themselves, and no clear similarities with the reference compounds. Doping the sample with phosphorus did not induce any significant differences with gels containing no phosphorus. The neodymium concentration and the leaching solution flow rate had no effect on the local environment of neodymium, contrary to what was observed for cerium. The radial pseudo-distance distributions in the gels (Fig. 8) were identical for all the gels. As in the case of the glass, and unlike cerium, no second-neighbor contribution was observed between 3 and 4 Å (distances uncorrected for phase shift); this suggests that the second coordination sphere of neodymium consists mainly of light atoms (Si, Al, Ca) with scattered Nd-2nd neighbor distances. The X-ray diffraction patterns for the gels without P (Nd2a for instance) were fully amorphous (Fig. 5), whereas the P-doped gels revealed the same diffraction lines than Nd3 glass that can be attributed to a mixed calcium and neodymium oxide phosphate, as for Nd3 glass.

Postulating a single silicate site, even with two distinct oxygen shells, did not yield a proper fit of the gel spectra obtained by alteration of Nd1 and Nd2 glass. The EXAFS spectra of the gels might indicate the presence of neodymium hydroxide or neodymium carbonate. However, the solubility of $Nd(OH)_3$ is relatively high ($\sim 10^{-5}$ M) at the pH under which the gels were formed (pH $\sim$ 8), making its presence unlikely in the gel. Fitting Nd1ab and Nd2abc gel spectra with a single $Nd(OH)_3$, $Nd_2(CO_3)_3$ or $NdOHCO_3$ site did not give satisfactory results. A correct fit of the gel spectra was obtained (Fig. 10) by taking into account two sites: a silicate ($Nd_2Si_2O_7$) and a hydroxycarbonate ($NdOHCO_3$) site. A study of glass/solution systems [35] showed that at basic pH values, the Nd concentrations in solution were controlled by $NdOHCO_3$. Neodymium, like europium [3] and cerium, is thus present at two different sites in the gels but the nature of the sites depends on the rare earth element considered. The phase and amplitude used for the $NdOHCO_3$ site were calculated with the FEFF7 code. Conversely, the spectrum for the Nds gel, in which Nd was adsorbed rather than incorporated in the gel silicate network, was fitted with a single $NdOHCO_3$ site.

The increase in the total neodymium coordination number was identical for all five gels without P (Nd1ab and Nd2abc) and the number of first-neighbor oxygen

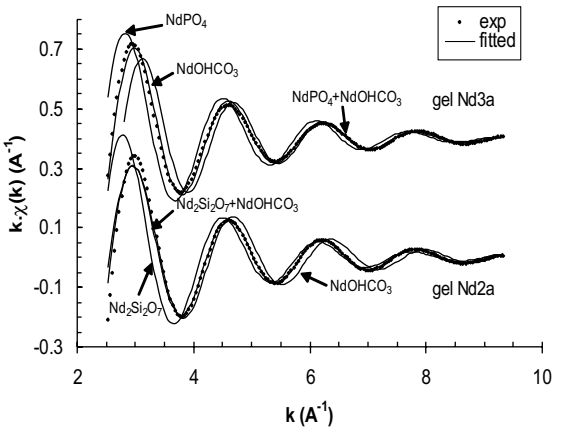

Fig. 10. Comparison between experimental and fitted EXAFS spectra for gels Nd2a and Nd3a.

atoms ranged from 9.0 to 9.4 (Table 8). The Nd–O distance for the silicate site increased to 2.54 Å (the distance was the same within 0.01 Å for all five gels). The ionic radii of Nd^{3+} are 1.109 Å at coordination number VIII and 1.163 Å at coordination number IX [24], a difference of 0.054 Å. During glass alteration the Nd–O distance increased by 0.06 Å for the silicate site, corresponding to the difference between the ionic radii of Nd^{3+}(VIII) and Nd^{3+}(IX). The modification of the local environment of the silicate site during glass alteration could thus be attributed to the change in neodymium ligancy, suggesting slight structural changes around the neodymium atom. Conversely, the $NdOHCO_3$-type site results from a much more extensive rearrangement of the neodymium local environment, as the mean length of the Nd–O bonds is 2.46 Å, slightly shorter in the gel than in the glass. A study of Nd-doped synthetic calcites ($CaCO_3$) [36] showed that the rare earth occupied a deformed calcium site with a coordination number of 7 and a Nd–O distance of 2.41 Å. This type of site differs from the site observed in our gels.

Although the leachate renewal rate does not affect the total neodymium coordination number or the Nd–O distances, it appears to modify the distribution of silicate and hydroxycarbonate sites in the gels. As for cerium, it is difficult to extract absolute value of coordination numbers when two types of sites are used to fit the spectra, but it is possible to give their evolution from one gel to another. The percentage of silicate sites in the gels increases from about 30% to 55% when the renewal rate decreases from 2/day to 1/week. So, neodymium presents the same behavior than cerium during Ce1 glass leaching. The silicate site in the gel would thus be very similar to the one in the glass, except for the longer Nd–O distance. In this case, the increase in the distance for this site could be due to the difference in the coordination number and to the fact that Nd occupies constrained sites in the glass and that relaxation occurred during alteration. The silicate-type sites in the gels could result from a simple in situ rearrangement (hydration) of the glass, whereas the $NdOHCO_3$-type sites could be formed by dissolution of the glass network followed by reprecipitation. The higher the glass alteration rate, the greater the restructuring resulting in the formation of the gels since the number of hydroxycarbonate sites increases with the gel formation rate. The neodymium concentration in the glasses and gels had no effect on its local environment, but this can be attributed to the fact that the concentration range investigated was considerably lower than the neodymium solubility limit in aluminoborosilicate glass [37].

Fitting the EXAFS spectrum of Nds gel (Table 8) gives a coordination number of 11 and a Nd–O distance of 2.45 Å, corresponding to the distance found in the gels with hydroxycarbonate sites. Within this assumption, the silicate site can be assigned to neodymium in the gel-forming silicate network, while the hydroxycarbonate site reflects simple adsorption of Nd on the gel. In this case, the adsorbed neodymium could be released during leaching of the gel.

As for gels Nd1ab and Nd2abc, two types of sites must be taken into account to obtain a proper fit of the Nd3ab gel spectra (Fig. 10), but with a phosphate-type site instead of a silicate-type site. The structural data for gels Nd3a and Nd3b are identical (Table 8). For the phosphate site, the Nd–O distance increased to 2.52 Å, and – within the measurement uncertainty tolerance – was the same as that of the silicate site in gels Nd1ab and Nd2abc, whereas the Nd–O distance for the hydroxycarbonate site was 2.40 Å. Compared with Nd3 glass, these values correspond respectively to a 0.10 Å increase and a 0.02 Å decrease in the Nd–O distance that cannot be attributed to a difference in ionic radii between Nd^{3+}(VII) and Nd^{3+}(VIII) [24].

The distribution of phosphate and hydroxycarbonate sites was identical for both gels Nd3ab and was not dependent on the leachate renewal rate used to fabricate the gels – contrary to the behavior observed for the gels without phosphorus. The phosphate-type site in the gels thus could result from an in situ rearrangement around Nd, while the $NdOHCO_3$-type site could be formed by dissolution followed by precipitation. The fact that the number of phosphate sites did not vary with the leaching conditions could indicate greater leaching stability for this type of site compared with silicate sites; this is consistent with the great thermodynamic stability of rare earth phosphates.

Neodymium was found at coordination number 7 in the Ndsp gel with an Nd–O distance of about 2.46 Å, i.e. the same distance as for Nd adsorbed on the gel without phosphorus (but with a lower coordination number). There is no evidence to indicate that the hydroxycarbonate site in the Nd3ab gels can correspond

to adsorption, as in the case of the gels without phosphorus.

5. Conclusion

The local environments of neodymium and cerium in gels obtained by pseudo-dynamic alteration of simplified (9-element) SON68-type glass samples were studied by XAS. The evolution of the local environment of neodymium and cerium after glass alteration was determined versus the leachate renewal rate.

In the glasses, cerium, mainly at oxidation state III, occupies a single silicate site in the glass. In the gels, cerium, only at oxidation state IV, occupies two sites: a silicate site and an oxide or more probably an oxyhydroxide site. The cerium local environment in the gels depends on the alteration conditions, the starting Ce^{4+}/Ce^{3+} ratio, and the Ce concentration in the glass. As a general rule, the gels obtained with a high leachate renewal rate exhibit higher total coordination numbers than ones obtained at low flow rate. In all the gels, cerium is present mainly in a silicate site and the Ce–O distances are almost constant from one gel to another. The differences in the Ce–O distances between glasses and gels cannot only be attributed to the variation of the ionic radii ($Ce^{3+} \rightarrow Ce^{4+}$) due to oxidation of Ce^{3+} from the glass. The sites occupied by cerium in the gels result from a major reorganization of the cerium local environment, affecting both the silicate and oxide sites. Upon leaching, for the glass of low cerium content, the quantity of silicate sites increases when the flow rate decreases. For the glasses of high cerium content, this quantity is constant versus the renewal rate. Gels formed with high renewal rates exhibit a Ce–Ce contribution, indicating that a fraction of the cerium incorporated in the gel is found in well ordered and highly cerium-enriched phases.

In the glasses without phosphorus, neodymium occupies a single silicate site. When the glass is doped with phosphorus, neodymium occupies a single phosphate site, although silicon is the major component of the glass. However, it is still unclear whether this lanthanum phosphate phase is completely or partially incorporated in the silicate network or whether it is an independent phase dispersed in the materials. After glass alteration, two different types of sites are occupied by neodymium. One is a silicate or phosphate, depending on whether the glass is doped with phosphorus or not, and the other one is a hydroxycarbonate site ($OHCO_3$). In the gels, the silicate and phosphate sites undergo slight structural changes (the coordination numbers remain unchanged and the Nd–O distance slightly increases), whereas the hydroxycarbonate site is more significantly reorganized. The leaching solution flow rate during glass alteration has no effect on the total neodymium coordination number or on the Nd–O distances, but modifies the percentages of silicate and hydroxycarbonate sites. In gels containing no phosphorus, the percentage of silicate sites increases when the leachate renewal rate diminishes from 2/day to 1/week. Conversely, in phosphorus-doped gels, the leaching solution flow rate does not affect the percentages of phosphate and hydroxycarbonate sites. The Nd_2O_3 concentration in the glass (up to 4 wt%) has no influence on the neodymium coordination number, the Nd–O distances, or the percentages of the two sites the gels. In any case, no Nd–Nd contribution is visible and consequently there are no aggregates of Nd-enriched phases in the gels. Neodymium could be trapped in the gels by two mechanisms: a fraction of the neodymium could be incorporated in the gel silicate network by in situ reorganization of the glass silicate sites, and another fraction could result of the coprecipitation of neodymium ($OHCO_3$ site).

Cerium and neodymium exhibit different leaching behavior and different sensitivity to the alteration conditions, although both elements have very similar chemical properties and identical retention factors in the gels. Cerium and neodymium are generally used as surrogates for plutonium and americium. This study demonstrates that caution is necessary with regard to the ability of cerium to simulate the leaching behavior of plutonium. For instance, in oxidizing media, plutonium shifts from valence IV in the glass to valence VI as plutonyl (PuO_2^{2+}) in the gel (PuO_2^{2+} will have a different local environment from Pu^{4+} or Ce^{4+}). By comparison with the local environments of some other chemical elements already determined through high-level waste containment glass alteration experiments, this study shows that the behavior of cerium and neodymium is intermediate between that of zirconium and iron. Zr is incorporated in the gel only by in situ reorganization while Fe is trapped only by coprecipitation.

Acknowledgement

The authors are grateful to the personnel of the LURE facility at Orsay where the XAS spectra were acquired.

References

[1] E. Pelegrin, PhD thesis, University of Paris VII, 2000.
[2] S. Ricol, PhD thesis, University of Paris VI, 1995.
[3] N. Ollier, G. Panczer, B. Champagnon, G. Boulon, P. Jollivet, J. Lumin. 94&95 (2001) 197.
[4] N. Ollier, M.J. Guittet, M. Gautier-Soyer, G. Panczer, B. Champagnon, P. Jollivet, Opt. Mater. 24 (2003) 63.
[5] P. Jollivet, C. Den Auwer, E. Simoni, J. Nucl. Mater. 301 (2002) 142.

[6] J.G. Darab, H. Li, M.J. Schweiger, et al., Pu Futures – The Science – Transuranic Waste, Santa Fe, USA, 1997, p. 143.
[7] E.A. Kuemmerle, G. Heger, J. Solid State Chem. 147 (1999) 485.
[8] N. Milinski, B. Ribar, M. Sataric, Crystal Struct. Commun. 9 (1980) 473.
[9] S. Violotis, A. Rimsky, Acta Crystallogr. B 31 (1975) 2620.
[10] A.C. Tas, M. Akinc, J. Am. Ceram. Soc. 11 (1994) 2968.
[11] A.L. Ankudinov, J.J. Rehr, Phys. Rev. B 56 (1997) 1712.
[12] J. Boucherle, Acta Crystallogr. B 31 (1975) 2745.
[13] G.W. Beall, W.O. Milligan, D. Dillin, R. Williams, J. McCoy, Acta Crystallogr. B 32 (1976) 2227.
[14] H. Dexpert, P. Caro, Mater. Res. Bull. 9 (1974) 1577.
[15] R.C. Mooney, Acta Crystallogr. 3 (1950) 337.
[16] N. Christensen, Acta Chem. Scand. 27 (1973) 2973.
[17] A. Michalowicz, J. Phys. IV (Paris) C 2 (1997) 235.
[18] J.A. Solara, J. Garcia, M.G. Proietti, Phys. Rev. B 51 (3) (1995) 2678.
[19] E. Fonda, D. Andreatta, P.E. Colavita, G. Vlaic, J. Synchrotron Radiat. 6 (1998) 34.
[20] S.A. Hayes, P. Yu, T. O'Keefe, M. O'Keefe, J. Electrochem. Soc. 149 (12) (2002) C623.
[21] L. Douillard, M. Gautier, N. Thromat, J.P. Duraud, Nucl. Instrum. and Meth. B 97 (1995) 133.
[22] S. Quartieri, F. Boscherini, et al., Phys. Chem. Miner. 29 (2002) 495.
[23] J.G. Darab, H. Li, J.D. Vienna, J. Non-Cryst. Solids 226 (1998) 162.
[24] R.D. Shannon, Acta Crystallogr. A 32 (1976) 751.
[25] T.K. Sham, J. Chem. Phys. 79 (3) (1983) 1116.
[26] Y. Joo-Byoung et al., Bull. Korean Chem. Soc. 21 (3) (2000) 305.
[27] H. Li, L. Li, J.D. Vienna, M. Qian, Z. Wang, J.G. Darab, D.K. Peeler, J. Non-Cryst. Solids 278 (2000) 35.
[28] S. Sen, J. Non-Cryst. Solids 261 (2000) 226.
[29] H. Yamagushi, H. Takebe, Jpn. J. Appl. Phys. 38 (1999) 168.
[30] E.M. Larson, F.W. Lytle, P.G. Eller, et al., J. Non-Cryst. Solids 116 (1990) 57.
[31] T. Wolery, UCRL-MA-110662 PTI ed., 1992, LLNL.
[32] G. Mountjoy, J.M. Cole, T. Brennan, R.J. Newport, et al., J. Non-Cryst. Solids 279 (2001) 20.
[33] M. Karabut, G.K. Marasinghe, E. Metwalli, et al., Phys. Rev. B 65 (2002) 104206.
[34] P. Henderson, Rare Earth Element Geochemistry, 1984, p. 14.
[35] D. Rai, A.R. Felmi, R.W. Fulton, J.L. Ryan, Radiochim. Acta 58&59 (1992) 9.
[36] E.J. Elzinga, R.J. Reeder, et al., Geochim. Cosmochim. Acta 66 (16) (2002) 2875.
[37] C. Lopez, X. Deschanels, et al., J. Nucl. Mater. 312 (2003) 76.